AIP | Review of Scientific Instruments

Investigating fusion plasma instabilities in the Mega Amp Spherical Tokamak using mega electron volt proton emissions (invited)a)

R. V. Perez, W. U. Boeglin, D. S. Darrow, M. Cecconello, I. Klimek, S. Y. Allan, R. J. Akers, D. L. Keeling, K. G. McClements, R. Scannell, M. Turnyanskiy, A. Angulo, P. Avila, O. Leon, C. Lopez, O. M. Jones, N. J. Conway, and C. A. Michael

Citation: Review of Scientific Instruments **85**, 11D701 (2014); doi: 10.1063/1.4889736
View online: http://dx.doi.org/10.1063/1.4889736
View Table of Contents: http://scitation.aip.org/content/aip/journal/rsi/85/11?ver=pdfcov
Published by the AIP Publishing

Investigating fusion plasma instabilities in the Mega Amp Spherical Tokamak using mega electron volt proton emissions (invited)[a)]

R. V. Perez,[1,b)] W. U. Boeglin,[1] D. S. Darrow,[2] M. Cecconello,[3] I. Klimek,[3] S. Y. Allan,[4] R. J. Akers,[4] D. L. Keeling,[4] K. G. McClements,[4] R. Scannell,[4] M. Turnyanskiy,[5] A. Angulo,[1] P. Avila,[1] O. Leon,[1] C. Lopez,[1] O. M. Jones,[4,6] N. J. Conway,[4] and C. A. Michael[7]
[1]*Department of Physics, Florida International University, 11200 SW 8 ST, CP204, Miami, Florida 33199, USA*
[2]*Princeton Plasma Physics Laboratory, James Forrestal Campus, P.O. Box 451, Princeton, New Jersey 08543, USA*
[3]*Department of Physics and Astronomy, Uppsala University, Uppsala SE-751 20, Sweden*
[4]*CCFE, Culham Science Centre, Abingdon, Oxfordshire OX14 3DB, United Kingdom*
[5]*ITER Physics Department, EFDA CSU Garching, Boltzmannstrasse 2, D-85748, Garching, Germany*
[6]*Department of Physics, Durham University, Durham DH1 3LE, United Kingdom*
[7]*Australian National University, Canberra ACT 0200, Australia*

(Presented 5 June 2014; received 31 May 2014; accepted 26 June 2014; published online 18 July 2014)

The proton detector (PD) measures 3 MeV proton yield distributions from deuterium-deuterium fusion reactions within the Mega Amp Spherical Tokamak (MAST). The PD's compact four-channel system of collimated and individually oriented silicon detectors probes different regions of the plasma, detecting protons (with gyro radii large enough to be unconfined) leaving the plasma on curved trajectories during neutral beam injection. From first PD data obtained during plasma operation in 2013, proton production rates (up to several hundred kHz and 1 ms time resolution) during sawtooth events were compared to the corresponding MAST neutron camera data. Fitted proton emission profiles in the poloidal plane demonstrate the capabilities of this new system. © *2014 AIP Publishing LLC*. [http://dx.doi.org/10.1063/1.4889736]

I. INTRODUCTION

Fast ion redistribution caused by electromagnetic field fluctuations could affect the performance of plasmas in the ITER burning plasma device, currently under construction. Diagnostics providing cost-effective, high time and spatial resolution of fast ion density profiles are essential for studying high frequency, short-time scale MHD plasma instabilities. A precedent exists for using collimated silicon detectors in conventional tokamak fast ion experiments to measure emission profiles.[1,2] Energy spectra were obtained for 3 MeV fusion protons (from Deuterium-Deuterium, or DD, fusion reactions) detected in the Princeton Large Torus and Axially Symmetric Divertor Experiment.[3–5] Spherical tokamak fast ion diagnostics such as the Mega Amp Spherical Tokamak (MAST) Neutron Camera[6] (NC) use 2.5 MeV DD fusion neutrons to infer emission profiles, while the MAST Fast Ion Deuterium Alpha (FIDA) spectrometer,[7] National Spherical Torus Experiment (NSTX) FIDA[8] spectrometer, and NSTX solid state neutral particle analyzer[9] observe charge exchange interactions, to study fast ion distributions during plasma MHD instabilities.

A prototype diagnostic to detect 3 MeV DD fusion protons in a spherical tokamak[10] has been installed in MAST at the Culham Centre for Fusion Energy (CCFE) in Culham, the United Kingdom. A compact, four-channel system of collimated silicon detectors where each detector probes a different region of the plasma, detects charged fusion products emitted along curved trajectories. This diagnostic takes advantage of the unconfined nature of 3 MeV protons and 1 MeV tritons from DD fusion reactions during the neutral beam injection (NBI) to create proton emission profiles. The capability of this prototype diagnostic to infer the proton emissivity during fast MHD events such as sawteeth is presented.

II. PROTON DETECTOR DESIGN

A. Charged fusion product trajectories

The PD's curved sightlines were reconstructed from an orbit code that calculates particle trajectories backwards in time from the point where they hit one of the PD's detectors. The curved integration paths for the DD charged fusion product trajectories, or orbits, depend on the MAST equilibrium magnetic field configuration reconstructed with EFIT[11] (an isotropic DD cross section is assumed). With a toroidal magnetic field between 0.5 T and 0.6 T, the 3 MeV proton and 1 MeV triton's gyro radii are of the order of 1 m, leaving them essentially unconfined by the plasma's magnetic field, and allowing them to leave the plasma before completing a full gyro-orbit. Equatorial and poloidal orbit projections (shown in Figs. 1 and 2) were used to determine the necessary angular orientation, with respect to the center of the MAST vessel, to probe different parts of the plasma core for each detector. Of the charged fusion products from the DD reaction, the protons and tritons have the same orbits while the helium-3 ions have considerably smaller gyro radii, completing ten

[a)]Invited paper, published as part of the Proceedings of the 20th Topical Conference on High-Temperature Plasma Diagnostics, Atlanta, Georgia, USA, June 2014.
[b)]Electronic mail: rvale006@fiu.edu.

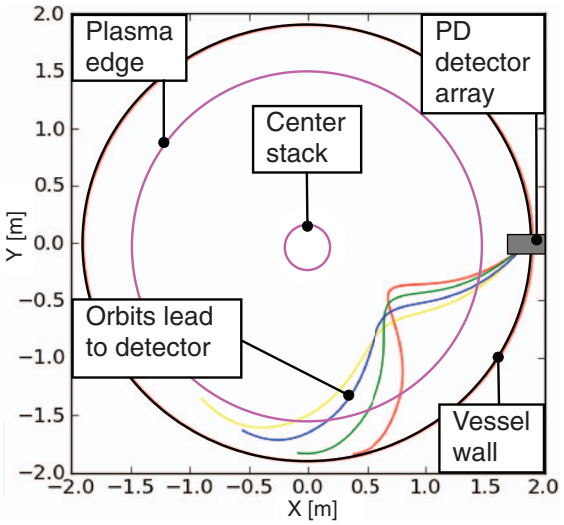

FIG. 1. The equatorial cross section of the MAST vessel with central orbit projections (in the PD coordinate system).

or more gyro-orbits before leaving the plasma. The plotted trajectories show the central orbits for each detector. Each of the four central orbits has a bundle of orbits which are dependent on the finite dimensions, length and diameter, of the collimating system (described in Sec. II B). The range of radial positions at the midplane sampled for one orbit bundle is ±3 cm from the plotted central orbit. Initial measurements for the detector-collimator system's solid angle acceptance are currently being carried out.

B. Mechanical housing

The PD stainless steel housing (Fig. 3(A)) connects to a mechanical probe arm that inserts the entire instrument,

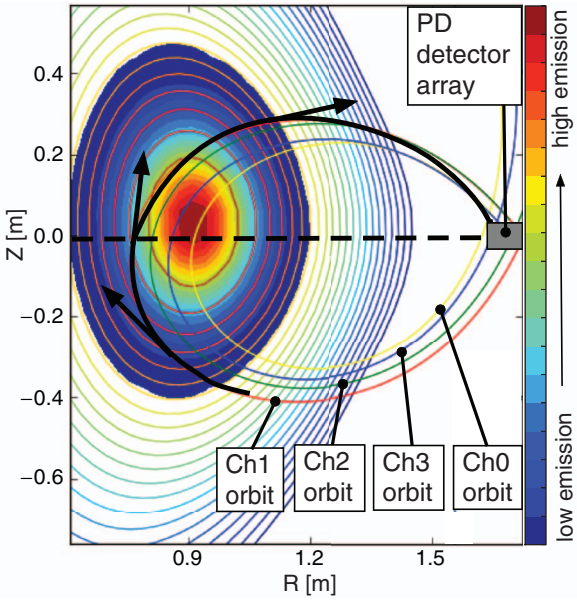

FIG. 2. Poloidal cross section of MAST with orbit projections. The PD detects particles with velocities tangential to the central orbits. The midplane radial intersections are the particle's R positions at Z = 0 m. The contour lines are surfaces of constant magnetic flux. Solid colors show the simulated proton emission.

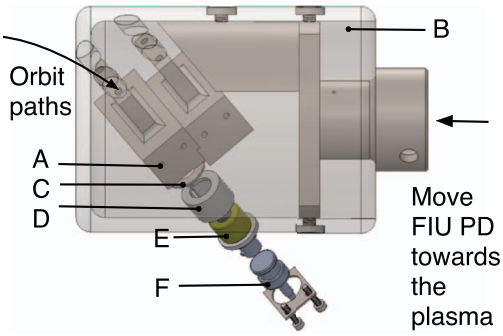

FIG. 3. Assembled PD is attached to a mechanical probe arm which inserts the entire diagnostic radially into the tokamak and towards the plasma. (A) Steel housing, (B) transparent shield, (C) Washer for foil attachment, (D) PEEK sleeve, (E) Detector, (F) Signal cable connection.

110 mm in diameter and 185 mm in length, through a 12.7 cm porthole into MAST's midplane. A 6 mm thick boron nitride (BN) ceramic shield (Fig. 3(B)) offers thermal and electrical insulation protecting the four detectors (Fig. 3(E)) and associated electrical components. The housing contains a 38 mm long collimator with a 3.8 mm diameter leading to the detector's 100 μm thick active layer. An 0.8 μm thick Aluminum foil (spot welded to a shim stock washer, Fig. 3(C)) was used to filter out soft x-rays and light emitted from the plasma. The energy loss for the proton, triton, and helium-3 ions passing through the foil were 18.4 keV, 34.6 keV, and 282 keV, respectively. A 1.8 mm thick Ketron PEEK 1000 sleeve (Fig. 3(D)) electrically insulates the gold-plated detector and its cable connection (Fig. 3(F)) from the rest of the steel housing. Note that a placement pin near the point of attachment of the PD to the mechanical probe arm ensured proper detector orientation after installation.

C. Data acquisition system

In each of the four data channels, the Ortec CU-014-050-100S silicon surface barrier detectors (intrinsic energy resolution of 14 keV) were attached to coaxial connectors of Accu-Glass Products, Inc.-TYPE25 Ultra High Vacuum (UHV) Kapton-coded coaxial cables. The detector's current signals passed through two custom connectors to the pre-existing UHV cables inside of the mechanical probe arm shaft. The connector thickness, crimping, and grounding methods used to create the connector resulted in a 30 mm distance of unshielded parallel signal cables. The signal left the probe arm shaft through two more custom connectors to Canberra 2003BT charge sensitive preamplifiers, where it was converted to a voltage proportional to the accumulated charge. LMR-195 coaxial cables were used for airside signal cables. The voltage signal was then amplified and shaped by a Canberra 2111 timing filter amplifier and digitized in a NI-PCI5105 high-speed digitizer. The digitizer, which collects 60 MSamples/s and has a 512 MB onboard memory, was installed on an Adnaco-S2 PCI Expansion System which was connected to a Supermicro 5016I-MTF server through an Adnaco-FC1 fiber patch cable. A program was written in LabVIEW 2011 to automate the digitizer's data collection.

A distance of about 3 m between the detectors and preamplifiers, the use of non-coaxial electrical feedthroughs, and

the grounding scheme for the system contributed to relatively high noise levels on the order of 0.1 V–0.15 V (five times higher than expected) with data signals ranging from 0.15 V to 1 V. These factors can be mitigated to reduce contributions to background noise levels for future diagnostic installations.

III. RAW DATA COLLECTION AND ANALYSIS

The diagnostic was installed and operated at MAST (at the CCFE) from August to September 2013. It was used, together with the NC and FIDA spectrometer, in dedicated fast particle physics experiments involving both the classical behavior of beams in the plasma and the effect of plasma instabilities on fast ions. The focus of this paper will be on sawtooth events in which the plasma's toroidal magnetic field (at the magnetic axis) was 0.58 T, plasma current was 600 kA, and NBI heating power was 1.3 MW. During these experiments the PD radial position along the major radius was remotely changed between plasma pulses to move towards and away from the center of the tokamak. The option for manual rotation of the PD about the major radius was not used. A digital trigger sent from the MAST Central Controller was configured in such a way that the PD collected 0.67 s of data per shot, or pulse (where a typical plasma pulse lasted up to 0.5 s).

Fusion proton signals are immediately evident at the beginning of the NB power (see Fig. 4), showing a clear dependence of signals on NBI heating and beam-thermal fusion reactions in MAST plasmas. The average particle signals seen in Fig. 5 have a width of about 100 ns, with protons peak heights around 0.6 V and triton peak heights around 0.2 V. Further studies are necessary to try to resolve helium-3 ions as their peak height of 0.15 V is on the order of the noise levels. 5.49 MeV alpha-decay from a ^{241}Am source was used to setup and test the equipment before and during installation to calculate expected signal ranges (see Fig. 6). Source pulse heights from 1.0 V to 1.3 V in the PD data acquisition system correspond to expected proton and triton signal ranges of 0.55 V–0.71 V and 0.18 V–0.24 V, respectively.

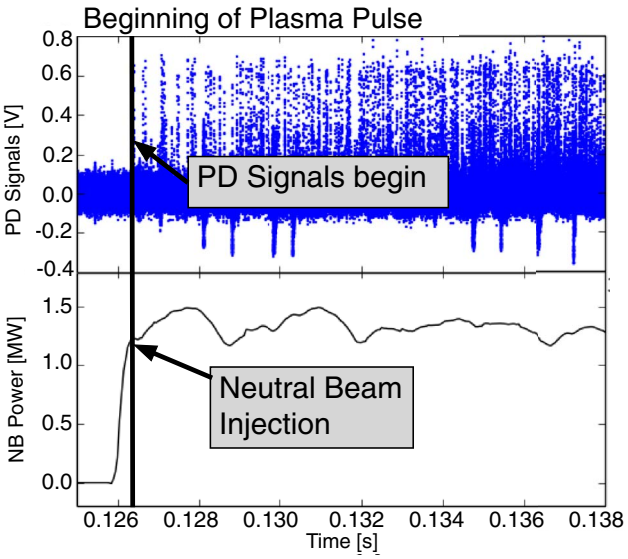

FIG. 4. Plasma pulse 29879, Ch2. Fusion proton signals appear as soon as the NBI heating is applied due to the beam-dominated nature of fusion reactions on MAST.

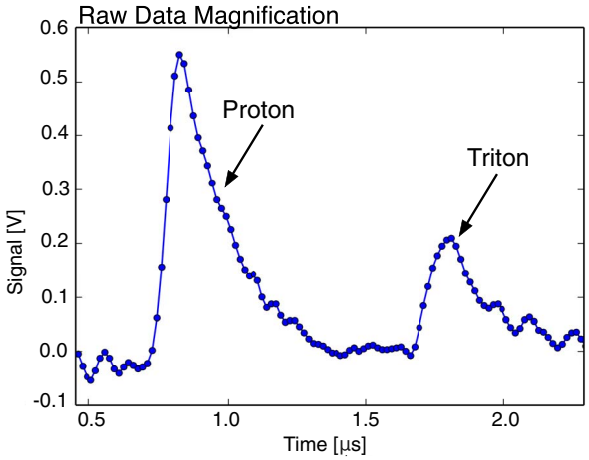

FIG. 5. Plasma pulse 29879, Ch 1. A magnification of data signals showing the characteristic shape of a fusion proton and triton. This finite time interval is not with respect to the beginning of the pulse.

Analysis software written in Fortran and Python was used to distinguish between real events and noise signals. Charged particles with an energy between 1 MeV and 3 MeV produce the same peak shape albeit with a different height. A normalized standard peak shape has been determined for each channel which could be expressed as

$$V = (V_0)\exp(-c_1(t + t_0))(1 + \tanh(c_2(t + t_0))), \qquad (1)$$

where V_0 is a calculated normalization factor, and c_1, c_2, and t_0 are parameters fitted to a set of sample peaks from each channel. Individual particle pulses with a height above a minimum threshold are then fitted on top of a quadratic background for a set of time ranges covering the entire data period (see Fig. 7). During this procedure, the peak positions are fixed and the fitted pulse amplitude is proportional to the particle energy. A particle energy spectrum is obtained by histogramming the fitted pulse amplitudes and makes it possible

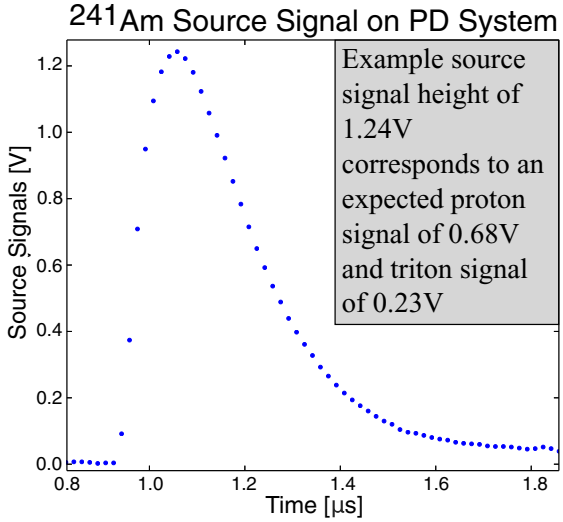

FIG. 6. Source signal due to a 5.49 MeV alpha-particle from the decay of a ^{241}Am source, used to test the PD system settings to calculate expected signal ranges for protons and tritons.

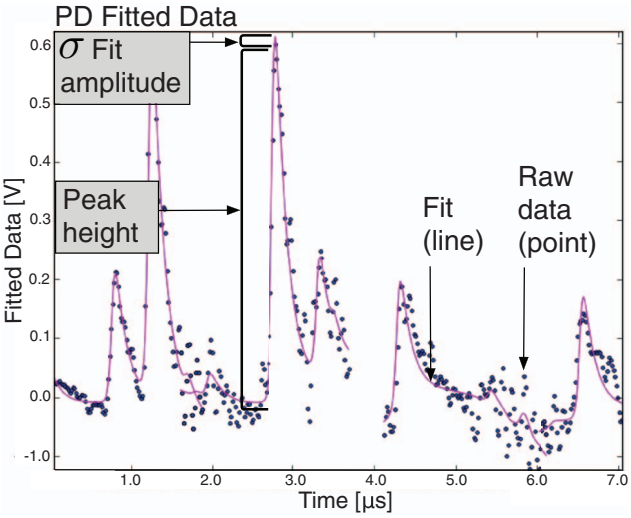

FIG. 7. Plasma pulse 29958, Ch2. A short time interval, not with respect to the beginning of the pulse, showing fitted data signals.

to identify the various particle types. Criteria used to reduce low energy and noise signals includes adjusting the value of a figure of merit (CR), where

$$CR = \sigma\, Fit\ amplitude / Peak\ height \qquad (2)$$

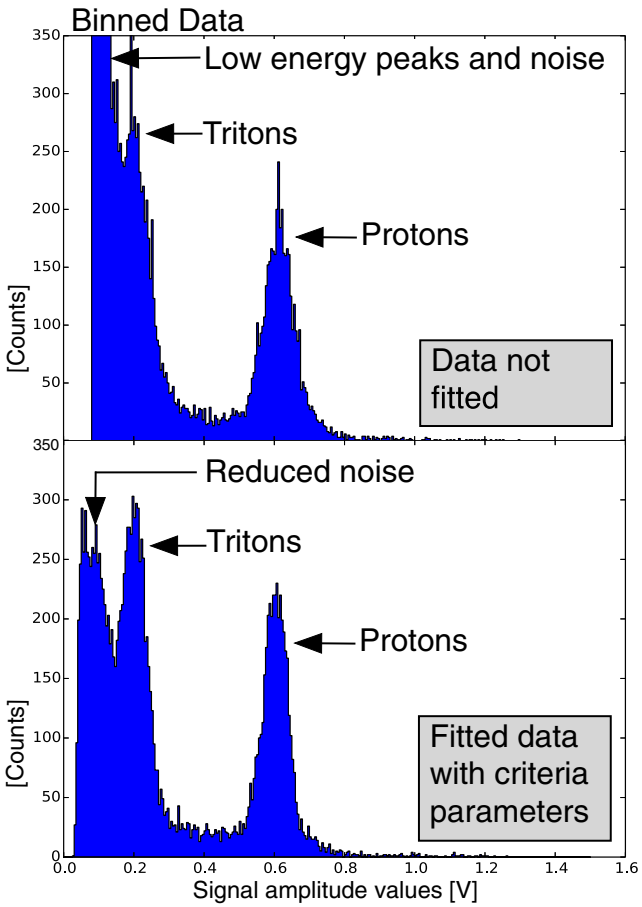

FIG. 8. Plasma pulse 29879, Ch2, time interval = 140 ms-210 ms. Effects of using criteria parameters on fitted data.

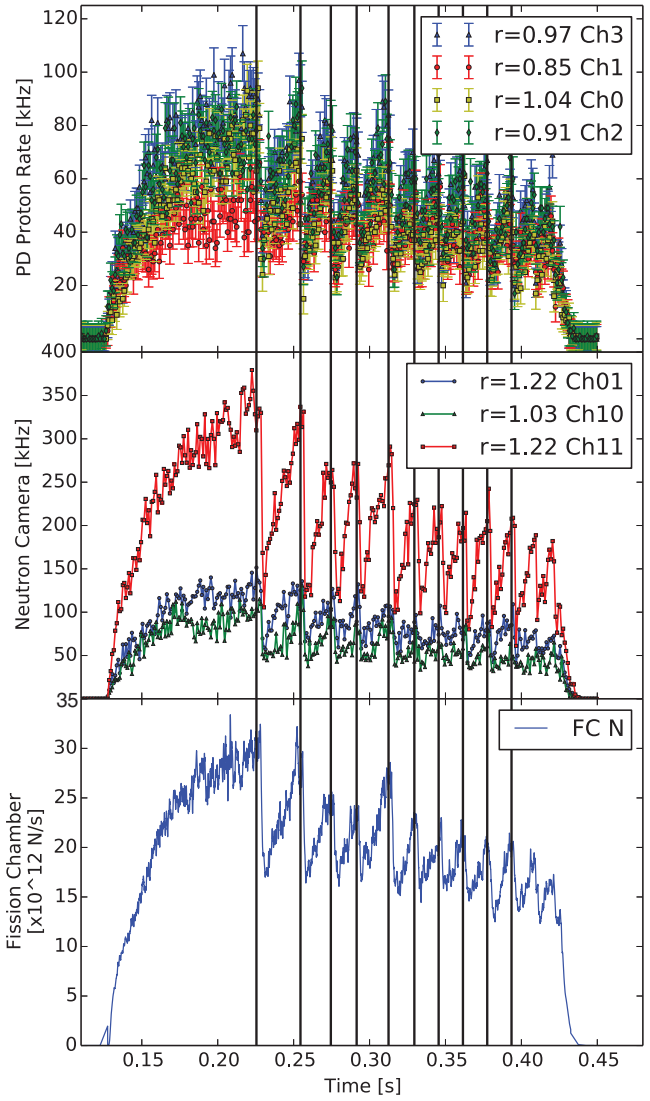

FIG. 9. Data for sawtooth crashes in plasma pulse 29879 from the PD, NC, and FC, where the units of labeled midplane radii are in meters.

as labeled in Fig. 7. A CR is individually chosen for each channel to suppress noise while avoiding excluding real events, resulting in a distribution where fusion tritons and protons are distinguishable (see Fig. 8). Histogram channels corresponding to proton signals are integrated to obtain the number of protons observed at the corresponding time interval (typical proton integration limits are from 0.5 V to 0.7 V). Ongoing work includes separating the triton signals from noise and low energy signals.

IV. FIRST RESULTS

A time resolution of 1 ms enables the observation of different plasma instability effects. Proton rates were extracted for plasma pulse, 29879, within a series of sawtooth-scenario repeated pulses. Fig. 9 highlights ten crashes from the PD, NC, and Fission Chamber (FC) data. For the purpose of demonstrating the PD's capabilities of creating radial profiles and emissivities, only the second crash at 254.5 ms will be further explored in this paper. Fig. 10 displays the radial

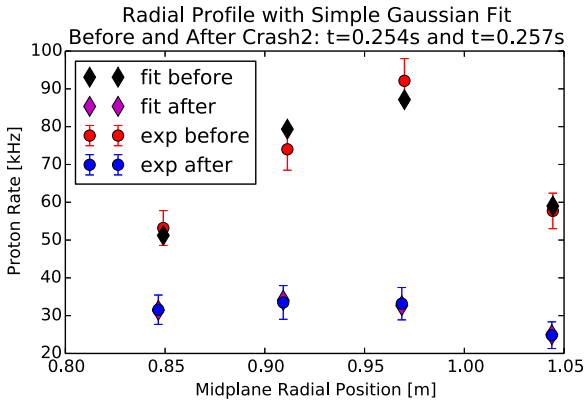

FIG. 10. Radial profile before the crash at t = 254 ms and after the crash at t = 257 ms during plasma pulse 29879.

profile, or proton emission as a function of the midplane radius before and after the crash. The poloidal orbits and fitted emissivities before and after the crash are plotted in Fig. 11. The function used to fit the emissivity to the observed proton rates is based on a simple gaussian,

$$S_g(r,z) = A\exp\left(((r-r_o)^2+z^2)/\sigma^2\right), \tag{3}$$

where S_g is the emissivity, r, z refers to the position in the R-Z plane (with respect to the magnetic axis), and A, r_0, and σ are fit parameters. In Fig. 12, each channel's emissivity is plotted as a function of the local value of ψ_{rel} (where ψ_{rel} is the magnetic flux relative to the magnetic axis and is defined in such a way that it is 1 at the magnetic axis and 0 at the plasma edge) for each coordinate (r,z) in Fig. 11. Following Channel 1's (red) orbit, it intersects the same flux surface at different points (r,z). The fitted emissivity has different values at these points even though the relative flux is the same. Consequently, the graphs in Fig. 12 are double valued. The range of emissivities for a given, fixed value of ψ_{rel} is a measure of the size of the emissivity variation on this flux surface. Continuing work includes fitting different functions to the experimental data.

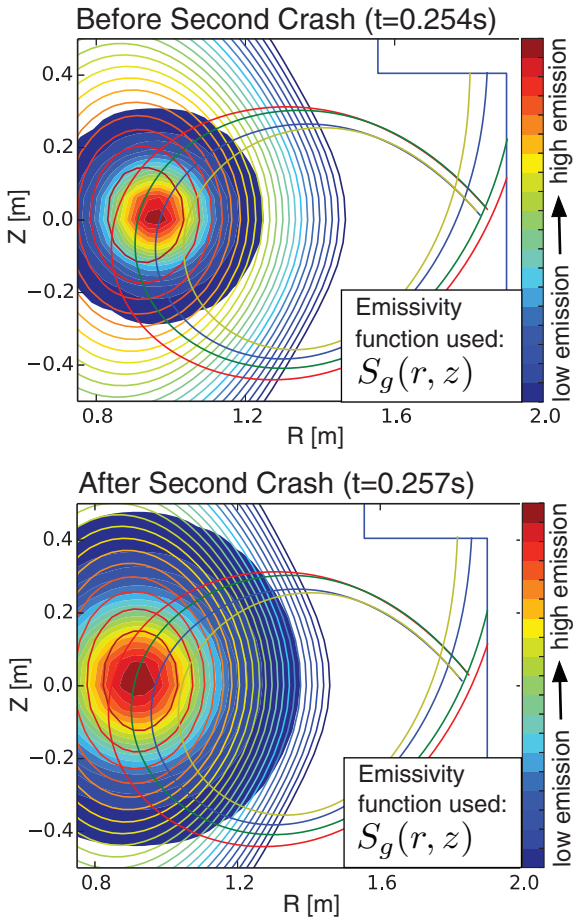

FIG. 11. Fitted emissivity profile before and after the second crash in pulse 29879.

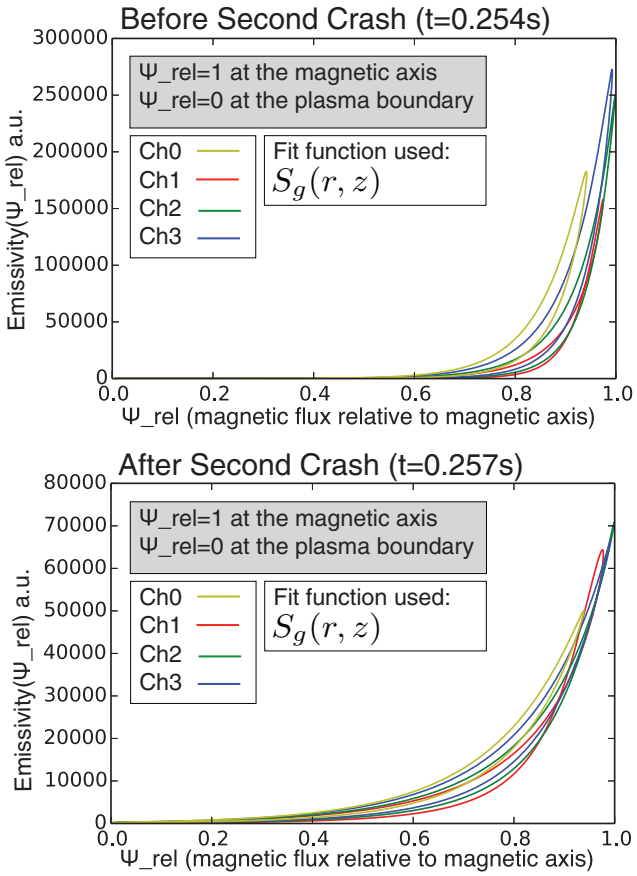

FIG. 12. Fitted emissivity plotted as a function of the poloidal magnetic flux before and after the second crash in pulse 29879.

V. SUMMARY

A proton detector on the MAST device has provided the first direct measurements of DD 3 MeV and 1 MeV fusion products in a spherical tokamak. Proton rates up to 200 kHz have been measured with a 1 ms time resolution during MHD plasma instabilities. Planned investigations include analysis of proton energy spectra for signs of thermal and non-thermal peak width broadening and its relation to the plasma ion temperature. Further work will include creating emission profiles by a combined PD and NC analysis, comparison to TRANSP fast ion distributions, and participating in a collaborative analysis of MHD events with the inclusion of MAST NC and FIDA diagnostics data. The PD's particle

energy resolution and dominant signal dependence on beam-thermal fusion events can provide information on the fast ion distribution, heating profile, and confinement of beam ions.

To construct more detailed emissivities, this prototype system can be scaled up into a larger 16-channel system to create model-independent proton and triton emission profiles. A PD array has the potential to provide information similar and complementary to a collimated neutron camera system in a more compact instrument, which will make it possible to employ a larger number of detector channels.

ACKNOWLEDGMENTS

This work was supported by: the (U.S.) Department of Energy (DOE) Contract Nos. DESC0001157 and DEAC0209CH11466 , the RCUK Energy Programme under Grant No. EP/I501045, the Swedish Research Council, the European Union's (EU) Horizon 2020 programme under Grant Agreement No. 210130335, the FIU Graduate & Professional Student Committee, and the FIU Ronald E. McNair Post-Baccalaureate Achievement Program. We would like to thank Nigel Thomas-Davies for his expertise during the PD installation. The views and opinions expressed herein do not necessarily reflect those of the European Commission.

[1]J. D. Strachan, Rev. Sci. Instrum. **57**, 1771 (1986).
[2]D. H. Lo, R. L. Boivin, and R. D. Petrasso, Rev. Sci. Instrum. **66**, 345 (1995).
[3]R. E. Chrien, R. Kaita, and J. D. Strachan, Nucl. Fusion **23**, 1399 (1983).
[4]W. W. Heidbrink and J. D. Strachan, Rev. Sci. Instrum. **56**, 501 (1985).
[5]H.-S. Bosch, Rev. Sci. Instrum. **61**, 1699 (1990).
[6]M. Cecconello *et al.*, Nucl. Instrum. Methods Phys. Res. A **753**, 72–83 (2014).
[7]O. M. Jones *et al.*, Plasma Phys. Control. Fusion **55**, 085009 (2013).
[8]M. Podestà *et al.*, Rev. Sci. Instrum. **79**, 10E521 (2008).
[9]D. Liu *et al.*, Rev. Sci. Instrum. **77**, 10F113 (2006).
[10]W. U. Boeglin, R. Valenzuela Perez, and D. S. Darrow, Rev. Sci. Instrum. **81**, 10D301 (2010).
[11]L. L. Lao *et al.*, Nucl. Fusion **30**, 1035 (1990).